Annals of Surgical Case Reports

Research Article
Published: 12 Jul, 2024

Quantitative Proteomic Analysis Provides Insight into the Therapeutic Mechanism of Horse Oil Percutaneous Permeation Treatment in a Rat Ankylosis Model

*Qianman B[1#], Jiasharete T[2#], Yeerjiang Y[3], Wupuer A[1],Tiangkejie W[4], Halpat A[1], Buranbai D[5], Jialihasi A[6], Shawutali N[7],Aihemaiti M[1], Maimaiti X[8], Alimujiang A[8], Tieliuhan T[9], Ydyrys A[10] , Aisaiding A[11], Yeerbo N[12] and Jielile J[1]**

[1]Department of Orthopedics & Ankle Surgery, The Sixth Teaching Hospital of Xinjiang Medical University, China

[2]School of Basic Medical Sciences, Capital Medical University, Beijing , China

[3]Department of Medical Records Management, The Sixth Affiliated Teaching of Xinjiang Medical University, China

[4]Qitai Hospital of the 6th Division, Xinjiang Production and Construction Corps, Qitai County, China

[5]Division of Child Neurology, Tottori University, Japan

[6]Department of Orthopedics, Almaty Medical Center HAK, Kazakhstan

[7]Department of Pediatric Surgery, The People's Hospital of Xinjiang Uygur Autonomous Region, China

[8]Department of Orthopedics Centre, The First Teaching Hospital of Xinjiang Medical University, China

[9]Department of Central Institutes of Health, Kupu Township, China

[10]Al-Farabi Kazakh National University, Biomedical Research Center, Kazakhstan

[11]Department of Hand and Foot Microsurgery, Children's Hospital of Xinjiang Uygur Autonomous Region, Urumqi, China

[12]Department of Geriatric Joint Surgery of Orthopedics, People's Hospital of Xinjiang Uygur Autonomous Region, Urumqi, China

[#]The authors contributed equally to this study

OPEN ACCESS

Correspondence:

Jiasharete Jielile, Department of Orthopedics & Ankle Surgery, The Sixth Teaching Hospital of Xinjiang Medical University, No. 39 Wuxing South Road, Urumqi, 830001, Xinjiang Uygur Autonomous Region, China, Tel: +86 18690216777;

Received Date: *04 Jun 2024*

Accepted Date: *06 Jul 2024*

Published Date: *12 Jul 2024*

Citation:

Qianman B, Jiasharete T, Yeerjiang Y, Wupuer A,Tiangkejie W, Halpat A, et al. Quantitative Proteomic Analysis Provides Insight into the Therapeutic Mechanism of Horse Oil Percutaneous Permeation Treatment in a Rat Ankylosis Model. Ann Surg Case Rep. 2024; 7(2): 1090.

Abstract

Background: The traditional medicine using Horse Oil Percutaneous Permeation (HOPP) has been recommended for the treatment of ankylosis. In this study, using a quantitative proteomics approach, we investigated the therapeutic mechanism of HOPP in a rat ankylosis model.

Methods: Sixty Sprague-Dawley (SD) rats with ankle joint ankylosis were randomized to a treatment group that received HOPP (n=30) or a control group (n=30). Synovial tissue samples from the ankle joint were collected at 7, 14, and 21 days in each group. Protein levels were assessed using isobaric Tags for Relative and Absolute Quantitation (iTRAQ). Differentially expressed proteins subjected to bioinformatics analysis.

Results: Among 1,729 proteins identified in synovial tissue samples, 200 proteins were differentially expressed across three time points between the HOPP treatment and control groups. Further analysis revealed that the differentially expressed proteins are involved in energy metabolism, calcium metabolism, myosin proteins, and mitogen-activated protein kinase signaling, and thus, these may represent the major mechanisms of the therapeutic effects of HOPP.

Conclusion: The results provide mechanistic insight into the improved joint function achieved with HOPP treatment, and thus, could be useful in the development of improved clinical treatments for anchylosis.

Keywords: Ankylosis; Arthrofibrosis; Traditional medicine; horse oil; iTRAQ; Proteomics; Therapeutic mechanism

Abbreviations

HOPP: Horse Oil Percutaneous Permeation; ROM: Functional Range of Motion; SD: Sprague–Dawley; PBS: Phosphate-Buffered Saline; PMSF: Phenylmethylsulfonyl Fluoride; DTT: Dithiothreitol; TFA: Trifluoroacetic Acid; SCX: Strong Cation Exchange; iTRAQ: Isobaric Tags for Relative and

Absolute Quantification; IPA: Ingenuity Pathway Analysis; MATLAB: Matrix and Laboratory; HESI: Heated Electrospray Ionization Source; ILK: Integrin Linked Kinase; GDI: Guanine Nucleotide Dissociation Inhibitor; MMPs: Matrix Metalloproteinases; HMMR: Hyaluronan-Mediated Motility Receptor; CSNK1G2: Casein kinase I isoform Gamma-2; PELO: Pelota (Drosophila) homolog; MAPK: The Mitogen-Activated Protein Kinase

Introduction

Ankylosis, or arthrofibrosis, is defined as joint pain and stiffness that prohibits functional Range of Motion (ROM) due to adhesions or contracture of the joint. Trauma and surgery are the most common etiological factors [1]. Arthrofibrosis is often caused by connective tissue proliferation, and the key pathological signs of arthrofibrosis are fibroblast proliferation along with collagen protein overexpression and aggregation, which lead to pain, swelling, stiffness, and the inability of the joint to move freely. Furthermore, mastocytes are also often observed in arthrofibrosis area. Growth factors and proteases secreted by mastocytes further contribute to fibroblast proliferation in the presence of calcium.

Arthrofibrosis is a common complication in orthopedics, with an incidence of up to 27%, and thus, a major cause of disability. Current therapies for arthrofibrosis have failed to achieve satisfactory results, particularly in the ankle joint [2-6]. There are many causes of ankle stiffness, among them: Achilles tendon rupture after fixation, can lead to ankle stiffness [7-9]. Treatment of tendon adhesions in arthrofibrosis is very difficult, and common approaches include herbal fumigation therapy combined with manipulation to release the adhesion as well as open operative methods [10].

Traditional Chinese medicine (Harbin Medical) treatment methods have amazing therapeutic effects on joint fibrosis or tendon adhesion [11-16]. Horse ointment or horse oil originated in China and has a history of over 4,000 years. The fatty acid content in horse oil is similar to that of human skin fat, so it can penetrate into the skin surface. Horse oil mainly contains some unsaturated acid groups, which have anti-inflammatory, antioxidant and scar-reducing effects [17-19]. Horse Oil Percutaneous Permeation (HOPP) is particularly recommended in traditional medicine as the best treatment for ankylosis [11-16,20]. HOPP shows amazing therapeutic effects on arthrofibrosis and tendon adhesions [10,16]. Our previous experience in clinical and laboratory experiments showed that application of HOPP can improve the ROM of the ankle joint in Sprague-Dawley (SD) model rats and facilitate joint reduction of chronic elbow or shoulder dislocation in humans [11,14-16].

In this study, we collected the synovial tissue from the ankle joint of the ankylosing SD rat model treated with HOPP and conducted proteome analysis in comparison with the ankylosing SD rat model. Quantitative proteomics methods were applied to find out the differential proteins between the groups. Informatics analysis was then performed to identify the functions of the differentially expressed proteins. The ultimate purpose of this study was to seek to elucidate the molecular therapeutic mechanisms of the HOPP in the SD rat ankylosis model and to identify the possible protein biomarkers of ankylosis healing.

Materials and Methods

Prepare of horse oil and surgical procedures

All protocols involving animals were approved by the Animal Ethics Committee of The First Teaching Hospital of Xinjiang Medical University (No: A-20180114012). All applicable international, national, and/or institutional guidelines for the care and use of animals were followed.

Horse oil was collected from a sacrificed 1-year-old horse (Yili, Xinjiang, China). The fat of the omentum was separated into many small pieces and snap freezes immediately before refinement by a carbon dioxide extraction method [21-25].

Using a table of random numbers, a total of 60 SD rats of the same age (8 weeks) and weight range (230 ± 20 g) were randomized to a HOPP-treated group (n=30) or a control group (n=30). The rats were anaesthetized by intraperitoneal injection of 10% lidocaine hydrochloride (5 ml/rat), and then tibia and fibula fractures were created closely in each rat using a bone breaking device [16]. After 5 days when the swelling was reduced, cast immobilization was applied with flexion of the knee joint at 75° and plantar flexion of the ankle joint at 0° for 7 weeks. After removal of the cast, 3 g of oil was applied on the outside of the rigid ankle joints of rats in the treatment group and secured by wrapping to prevent oil oxidation. The oil sheets (a piece of cotton) were replaced six times per day [15,16]. All rats were allowed free access to food and water, and rats in either group were excluded from the study if death, loosening of the plaster cast, or infection occurred [26,27].

Sample preparation, protein extraction, trypsin digestion, and isobaric tags for relative and absolute quantification (iTRAQ) labeling

At 7, 14, and 21 days after the initiation of HOPP treatment, rats in the two groups were sacrificed and 0.2 cm × 0.2 cm × 0.2 cm samples of synovial tissue were resected from the ankle joint under a surgical microscope (M525 F40 Leica, Germany). The samples were rinsed thoroughly three times with ice-cold Phosphate-Buffered Saline (PBS) to remove the blood [21-32]. After grinding in liquid nitrogen, samples were lysed with lysis buffer (7 M urea, 2 M sulfourea, 0.1% Phenylmethylsulfonyl Fluoride (PMSF), 65 mM Dithiothreitol (DTT)) for 30 min on ice according with a sample weight to lysis buffer volume ratio of 5:1 (w:v). Samples were then centrifuged at 20,000 g and 4°C, and the supernatant was saved for measurement of protein content. For trypsin digestion, 100 μg of crude proteins from each sample was reduced with 25 mmol/L NH_4HCO_3 containing 10 mmol/L DTT (Promega, USA) for 60 min at 60°C. Then a cystine blocking reagent was added to the samples for 10 min at room temperature. Afterwards, pre-cooled acetone was added to each tube at a sample to acetone ratio of 1:5 (v:v) for precipitation of the protein at -20°C for 60 min. Protein precipitates were collected by centrifugation at 20,000 g and 4°C for 20 min and then dissolved in 20 μL dissolution buffer. Trypsin was added to the samples according to a trypsin to protein ratio of 1:20 (w:w). After digestion overnight at 37°C, iTRAQ® labeling reagents (ABI, USA) dissolved in 70 μL of ethanol were added to each sample (HOPP-7d, iTRAQ® 113; HOPP-14d, iTRAQ® 114; HOPP-21d, iTRAQ® 115; control-7d, iTRAQ® 116; control-14d, iTRAQ® 117; and control-21d, iTRAQ® 118) for reaction for 2 h at room temperature. After labeling, the peptides were reconstituted in 0.1% Trifluoroacetic Acid (TFA), desalted with a Sep-Pak C18 column (Waters Corp., Miford, Massachusetts, USA), and then dried under vacuum before separation using two-dimensional liquid chromatography as described below.

Two-dimensional liquid phase chromatographic fractionation and tandem mass spectrometry analysis

The dried eluates were dissolved in Strong Cation Exchange (SCX) solvent A (10 mM KH_2PO_4, 25% acetonitrile, pH 2.6) and fractionated in a Shimadzu HPLC system LC20-AD using a polysulfoethyl column (2.1 mm × 100 mm, 5 µm, 200 Å; PolyLC, USA). The peptides were eluted at a flow rate of 200 µL/min with a linear gradient of 5% to 25% solvent B (10 mM KH_2PO_4, 350 mM KCl, 25% acetonitrile, pH 2.6) over 60 min. The absorbance at 214 nm/280 nm was monitored. Twenty fractions were collected based on peak intensities and then dried under vacuum. Each SCX fraction was dissolved in 50 µL solvent A (5% acetonitrile, 0.1% acetic acid) and further separated in the Shimadzu HPLC system LC20-AD using a ZORBAX 300SB-C18 column (5 µm, 300 Å, 0.1 mm × 15 mm; Agilent, USA) a flow rate of 60 µL/min. Peptides were eluted at a flow rate of 300 nL/min with a linear gradient of 5% to 35% solvent B (95% acetonitrile, 0.1% acetic acid) over 90 min.

For mass spectrometry analysis, a Q-Exactive Mass Spectrometer (Thermo Scientific, USA) was operated in positive ion mode with the Heated Electrospray Ionization Source II (HESI II). The HESI II conditions were: Spray voltage, 3800 V; sheath gas pressure (N_2), 35 arb; and capillary temperature, 320°C. Mass spectra were analyzed with Xcalibur software.

Protein identification and data analysis

The MS/MS data from the iTRAQ experiments were retrieved using Protein Discovery software (Thermo Scientific, USA) with search parameters as follows: SwissProt_Rat database, trypsin digestion, cysteine alkylation, and iTRAQ peptide labeling. The final fold change was determined relative to the corresponding controls from all replicates. A 2-fold increase or 0.5-fold decrease in the expression of identified proteins was considered significant differential expression. Statistical analysis of these data was performed with EXCEL (Microsoft, USA) and Matrix and Laboratory (MATLAB) software (MathWorks, USA). Ingenuity Pathway Analysis (IPA; http://analysis.ingenuity.com) was performed to identify the signaling pathways, protein–protein network, and target genes associated with the differentially expressed proteins.

Results

Total proteome of rat synovial tissue

Overall, 1,729 proteins were identified in the rat synovial tissue. Gene ontology analysis was performed to annotate the function of the identified proteins (http://geneontology.org/), and all identified proteins were assigned to functional categories according to biological processes (Table 1). The 10 most-represented categories were translational elongation, generation of precursor metabolites and energy, cellular carbohydrate catabolic process, glucose catabolic process, establishment of protein localization, protein transport, carbohydrate catabolic process, alcohol catabolic process, hexose catabolic process, and monosaccharide catabolic process. In addition, the identified proteins were assigned to functional categories according to cellular component (Table 2), and the 10 most-represented components were cytosol, cytosolic part, mitochondrion, mitochondrial part, soluble fraction, non-membrane-bound organelle, intracellular non-membrane–bound organelle, cytoskeleton, pigment granule, and melanosome.

Table 1: Biological processes of proteins identified as differentially expressed in synovial tissue from a rat model of ankylosis (TOP 10).

Biological process	P value	Pop Hits
Translational Elongation	2.29E-38	95
Generation of Precursor Metabolites and Energy	1.04E-27	238
Cellular Carbohydrate Catabolic Process	6.12E-20	72
Glucose Catabolic Process	1.99E-17	57
Establishment of Protein Localization	2.37E-17	554
Protein Transport	2.80E-17	549
Carbohydrate Catabolic Process	3.75E-17	98
Alcohol Catabolic Process	4.76E-17	72
Hexose Catabolic Process	8.29E-17	59
Monosaccharide Catabolic Process	8.29E-17	59

Table 2: Cellular components occupied by proteins differentially expressed in synovial tissue of rats with ankylosis after treatment with HOPP (TOP 10).

Cellular Component	P value	Top Hits
Cytosol	8.59E-69	1118
Cytosolic Part	2.33E-30	109
Mitochondrion	2.01E-28	1250
Mitochondrial Part	8.66E-25	515
Soluble Fraction	5.53E-24	298
Non-Membrane-Bounded Organelle	1.71E-23	1823
Intracellular Non-Membrane-Bounded Organelle	1.71E-23	1823
Cytoskeleton	3.33E-23	940
Pigment Granule	6.01E-23	73
Melanosome	6.01E-23	73

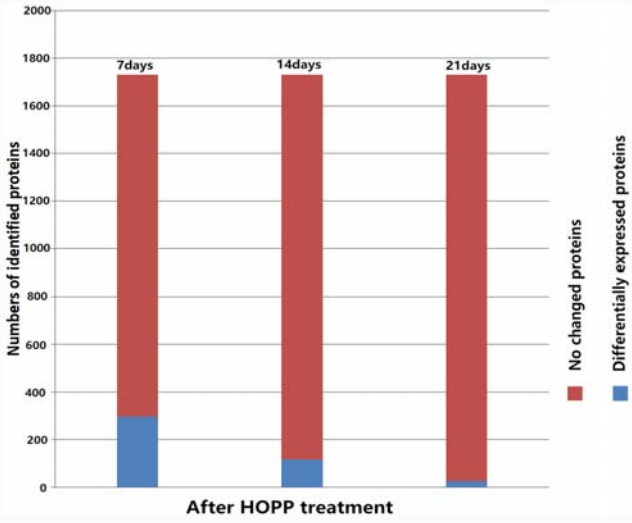

Figure 1: The proportions of differentially expressed proteins after HOPP treatment for different durations (7, 14, and 21 days).

Cluster analysis and functional annotation of proteins differentially expressed after HOPP treatment

Compared with that from the control group, synovial tissue collected from the HOPP treatment group differentially expressed 291 proteins (74 upregulated and 217 downregulated) at 7 days from the start of treatment, 238 proteins (91 upregulated and 147 downregulated) at 14 days, and 72 proteins (37 upregulated and 35

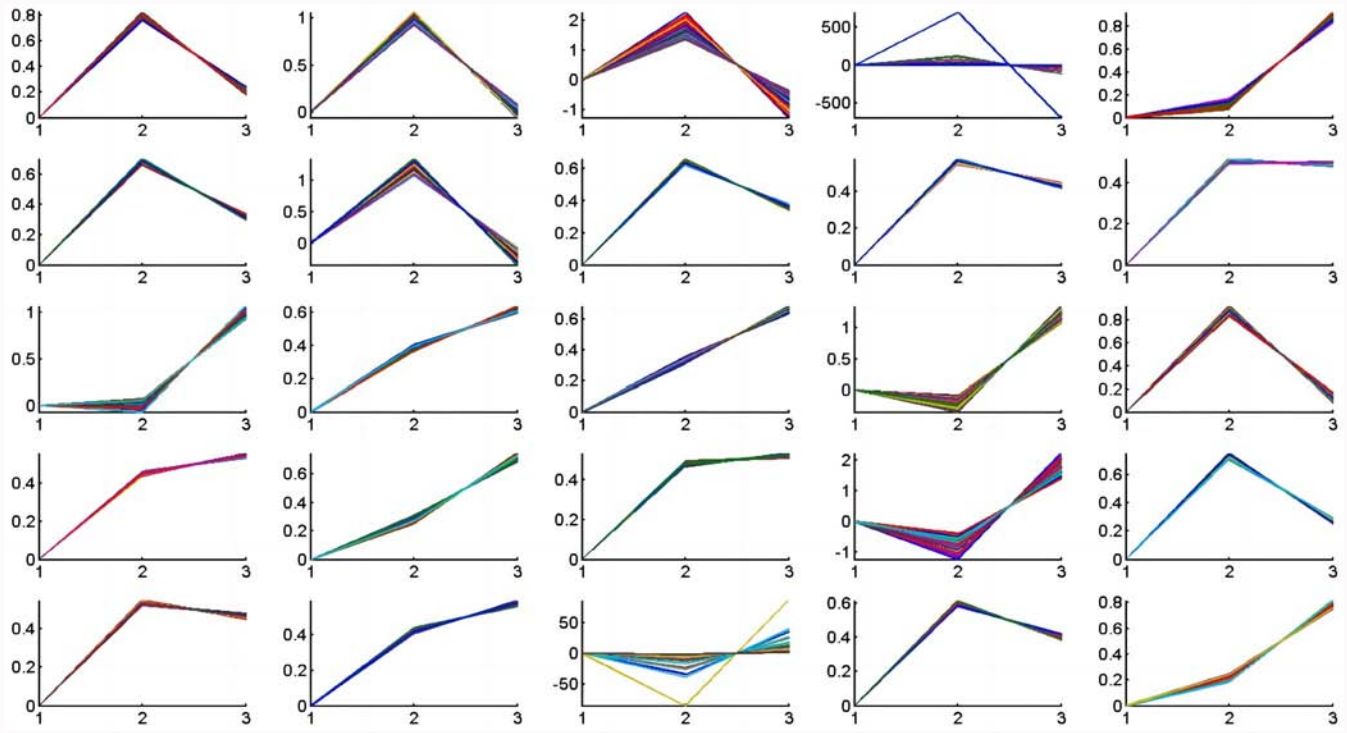

Figure 2: Cluster analysis of differentially expressed proteins after HOPP treatment. A total of alteration types was concluded. The x-axis corresponds to the different healing stages (1, 2, and 3 mark 7, 14, and 21 days, separately).

downregulated) at 21 days (Figure 1). These results revealed that the number of differentially expressed proteins gradually decreased as the time course of HOPP treatment increased (Figure 1).

Cluster analysis using the K-means analysis method was performed for the proteins differentially expressed after HOPP treatment. The proteins formed 25 clusters (Figure 2), which could be divided into three groups according to the change in expression during HOPP treatment: Continuously increasing expression, continuously decreasing expression, and fluctuating expression (Figure 2).

Gene ontology analysis was performed to annotate the function of proteins differentially expressed with HOPP treatment. All differentially expressed proteins were assigned to six functional categories according to biological processes (Figure 3A), which included generation of precursor metabolites and energy, cellular carbohydrate catabolic process, carbohydrate catabolic process, glycolysis, muscle system process, and striated muscle contraction. The differentially expressed proteins also were assigned to 10 functional categories according to molecular function (Figure 3B), which included cytoskeletal protein binding, actin binding, nucleotide binding, calmodulin binding, motor activity, identical protein binding, fructose binding, purine ribonucleotide binding, ribonucleotide binding, and purine nucleotide binding. Moreover, the differentially expressed proteins were assigned to four functional categories according to cellular component (Figure 3C), which included contractile fiber, myofibril, contractile fibers, and sarcomere.

Pathway analysis of differentially expressed proteins after 7 days of HOPP treatment

The pathways involving the proteins differentially expressed upon HOPP treatment were identified *via* IPA. As shown in Figure 4A, these pathways included calcium signaling, cellular effects of sildenafil, glycolysis I, protein kinase A signaling, tight junction signaling, Integrin Linked Kinase (ILK) signaling, epithelial adherens junction signaling, gluconeogenesis I, actin cytoskeleton signaling, and regulation of eIF4 and p70S6K signaling. Interestingly, it was the differentially downregulated proteins that mainly contributed to those pathways (Figure 4A). In addition, the differentially expressed proteins related to muscle contraction and Ca^{2+} signaling also were downregulated after 7 days of HOPP treatment (Table 3 and Figure 4B). We also analyzed the significantly enriched pathways and their crosstalk that involve the proteins differentially expressed after 7 days of HOPP treatment (Figure 4C).

Pathway analysis of differentially expressed proteins after 14 days of HOPP treatment

The proteins differentially expressed after 14 days of HOPP treatment were involved in the pathways of calcium signaling, ILK signaling, agranulocyte adhesion and diapedesis, actin cytoskeleton signaling, 3-phosphoinositide biosynthesis, cellular effects of sildenafil, epithelial adherens junction signaling, 3-phosphoinositide degradation, the superpathway of inositol phosphate compounds, and D-myo-inositol (1,4,5,6)-Tetrakisphosphate biosynthesis (Figure 5A). Notably, the differentially expression proteins related to muscle contraction and Ca^{2+} signaling that were downregulated after 7 days of HOPP treatment had begun to be upregulated (Table 3 and Figure 5B). Again, we analyzed the significantly enriched pathways and their crosstalk that involve the proteins differentially expressed after 14 days of HOPP treatment (Figure 5C).

Pathway analysis of differentially expressed proteins after 21 days of HOPP treatment

The proteins differentially expressed after 21 days of HOPP

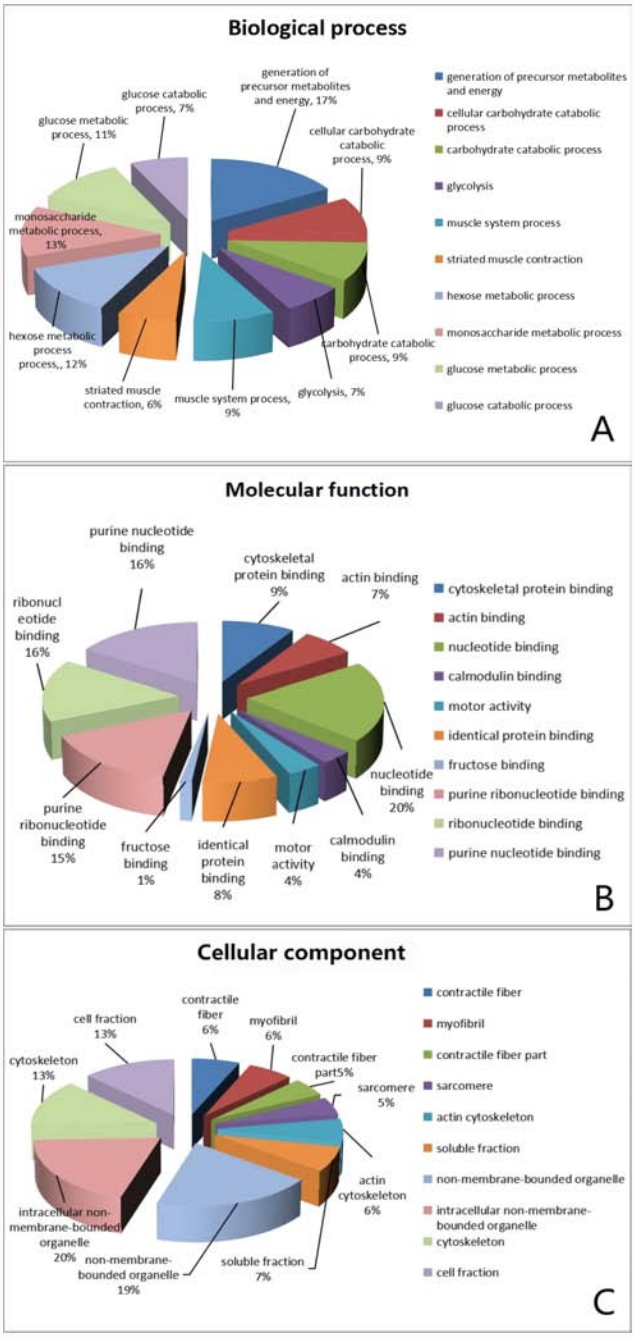

Figure 3: Pie charts showing the results of this gene ontology analysis of differentially expressed proteins. Different colors stand for different clusters. The corresponding cluster names are listed beside the pie chart. (A), biological process. (B), molecular function, and (C), cellular component.

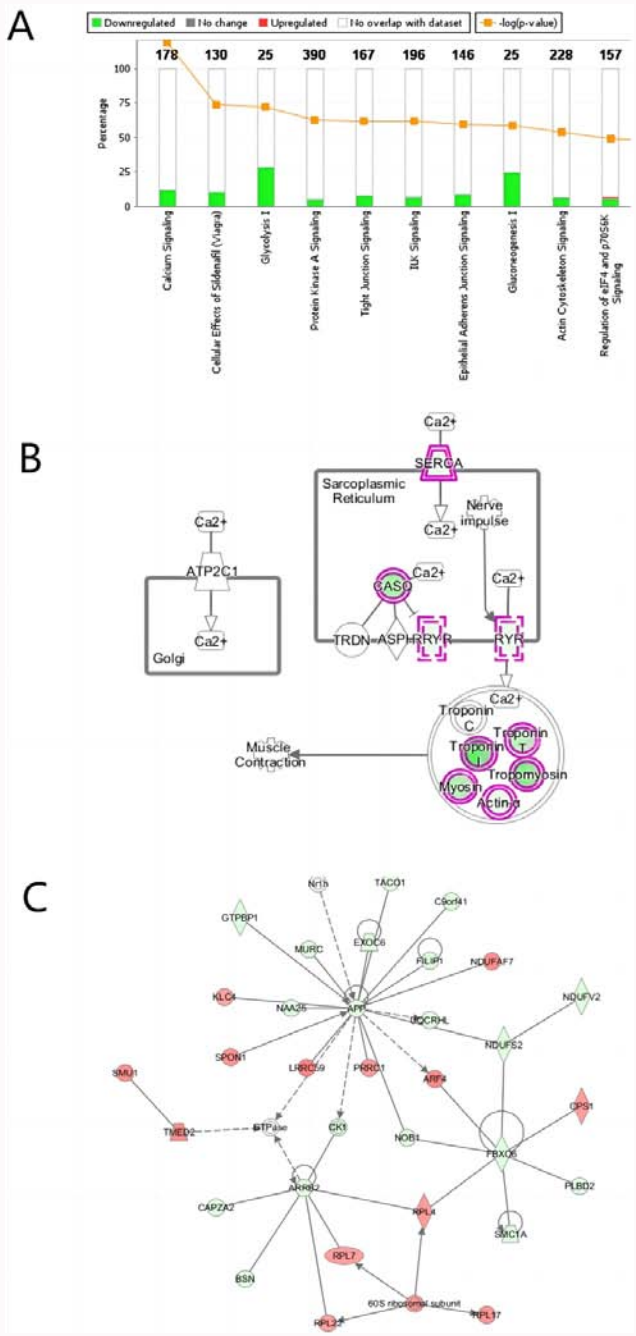

Figure 4: Pathway analysis of differentially expressed proteins at 7 days after HOPP treatment. (A) Analysis of pathway enrichment using IPA software. Green indicates the proportion of downregulated proteins; red stands indicates the proportion of upregulated proteins; white represents the proteins in the database that were not identified as differentially expressed in our study. The –log(p-value) serves as the units for the level of enrichment, and more enriched clusters often have a larger –log(p-value). (B) Analysis of function enrichment using IPA software. (C) Analysis of protein networks using IPA software. Different node types indicate the different patterns in protein expression alteration. Green nodes represent downregulated proteins, red nodes indicate upregulated proteins, and white nodes show the proteins that were not differentially expressed compared with the control. Lines among proteins indicate the relationships of these proteins.

treatment were involved the pathways of hepatic fibrosis/hepatic stellate cell activation, asparagine degradation I, protein ubiquitination pathway, epithelial adherens junction signaling, protein citrullination, aldosterone signaling in epithelial cells, Cdc42 signaling, RhoGDI signaling, mitotic roles of polo-like kinase, and calcium signaling (Figure 6A). Moreover, the expression levels of most of the proteins related to muscle contraction and Ca^{2+} signaling that were differentially expressed at the earlier time points now showed almost no difference compared with the expression levels in the control tissue (Table 3 and Figure 6B). Finally, we analyzed the significantly enriched pathways and their crosstalk that involve the proteins differentially expressed after 21 days of HOPP treatment and found that the pathways enriched after 21 days of HOPP treatment were completely different from those enriched after 7 and 14 days of HOPP treatment (Figure 6C).

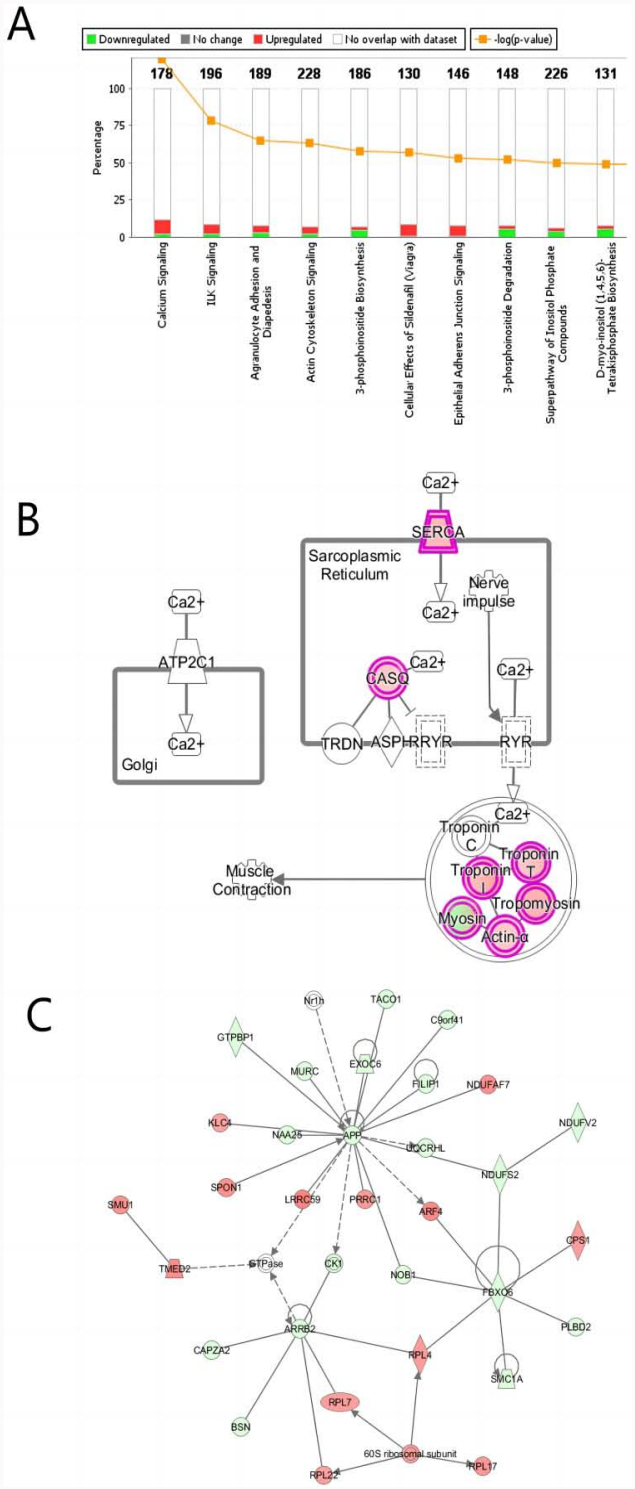

Figure 5: Pathway analysis of differentially expressed proteins after 14 days of HOPP treatment. (A) Analysis of pathway enrichment using IPA software. Green represents the proportion of downregulated proteins, while red indicates the proportion of upregulated proteins. White stands for the proteins in the database that, while not included in our study, have –log(p-value) values for the level of enrichment. Notably, more enriched clusters often have a larger –log(p-value). (B) Analysis of function enrichment using IPA software. (C) Analysis of protein networks using IPA software. Different node types indicate the different patterns in protein expression alteration. Green nodes indicate the downregulated proteins, and red nodes represent the up-regulated proteins. The white nodes reveal proteins that showed not significant alteration upon HOPP treatment. The lines among proteins indicate the relationships of these proteins.

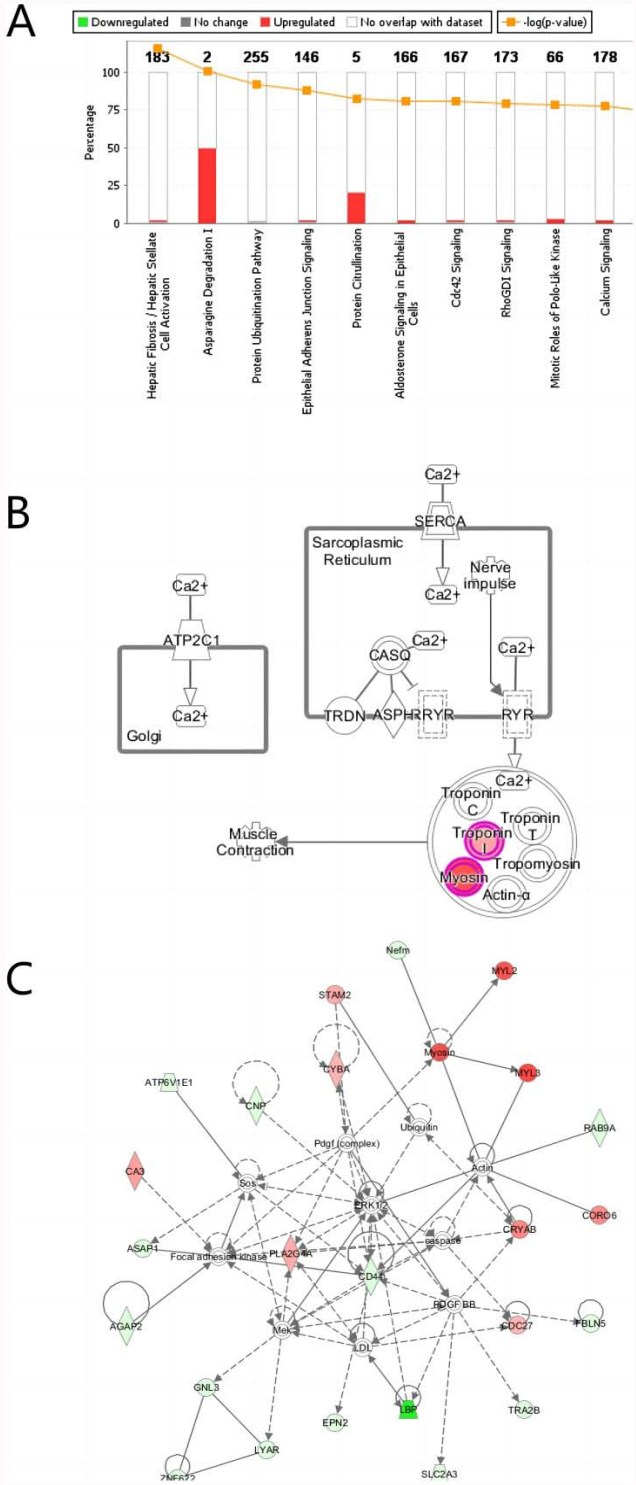

Figure 6: Pathway analysis of differentially expressed proteins after 21 days of HOPP treatment. (A) Analysis of pathway enrichment using IPA software. Green represents the proportion of downregulated proteins, whereas red stands for the proportion of upregulated proteins. Again, white indicates the proteins in the database that, although not identified in our initial study, have a –log(p-value) for enrichment. Notably, more enriched clusters often have a larger –log (p-value). (B) Analysis of function enrichment using IPA software. (C) Analysis of protein networks using IPA software. Different node types indicate different patterns in protein expression alteration. Green nodes indicate downregulated proteins, red nodes represent the upregulated proteins, and white nodes stand for proteins that showed no significant alteration compared with the control group. Lines among proteins indicate the relationships of these proteins.

Table 3: Fold change in expression of proteins related to muscle contraction and Ca^{2+} signaling at different time point after HOPP treatment.

Symbol	Exp Fold Change (7 Day)	Exp Fold Change (14 Day)	Exp Fold Change (21 Day)
ACTA1	-4.124	2.673	1
ATP2A1	-4.384	3.39	1
CALR	1	-2.01	1
CASQ1	-12.657	2.732	1
HDAC1	1	-2.246	1
MYH3	-4.716	3.894	1
MYH4	-6.003	3.863	1
MYH6	-6.42	4.214	1
MYH7	-8.567	4.062	1
MYH8	-5.169	4.299	1
MYH9	1	-2.07	1
MYL1	-10.417	3.428	1
MYL2	-6.356	2.365	4.786
MYL3	-8.415	2.959	5.127
TNNI1	-4.841	3.305	2.552
TNNI2	-19.637	5.047	1
TNNT1	-10.009	3.793	1
Tnnt3	-6.24	2.834	1
Tpm1	-15.631	3.761	1
Tpm2	-8.582	3.83	1

Discussion

Proteomics analysis based on large-scale, high-throughput separation and analysis technology has been used to identify proteins differentially expressed in various orthopedic conditions [21,22,33-48]. In the present study, we used iTRAQ-labeling quantitative proteomics to identify proteins that were differentially expressed in synovial tissue samples from a rat model of ankylosis following HOPP treatment in order to gain insight into the therapeutic mechanism of HOPP in arthrofibrosis.

Analysis of the main differential proteins between the HOPP-treated and non-treated ankylosis animal models showed that these proteins play a role in important biological processes related to sugar catabolism and protein transport (Table 1). Combined with the cellular distribution of these differential proteins by gene ontology analysis, they were mainly localized in the cytoplasm, especially in mitochondria, and non-membrane–bound organelles (Table 2). These localizations are also consistent with the site where sugar catabolism and protein transport processes occur. We know that inflammatory response is the key pathological mechanism that causes joint and bone fusion. Macrophages are osteoclast progenitor cells and play an important role in bone resorption. They are present during the inflammatory phase of fracture healing in humans and animals and play a key role in initiating fracture repair [39]. Macrophages eliminate pathogenic microorganisms, cell debris and necrotic tissue, and induce inflammatory factors such as interleukin 1, post-injury interleukin 6 and tumor necrosis factor-α to initiate an inflammatory response. Intracellular metabolic changes activate macrophage function. M1 macrophages increase glucose consumption and lactate release, and decrease oxygen consumption rates. M2 macrophages mainly use the oxidative glucose metabolism pathway. In addition, fatty acid, vitamin, and iron metabolism are also related to macrophage polarization [40]. HOPP treatment inhibits sugar metabolism and protein transport in the early stage of bone repair, being beneficial to reducing local inflammatory response.

From the molecular function analysis of the differentially expressed proteins, the most enriched protein clusters were cytoskeletal protein-binding clusters, including actin-binding and nucleotide-binding proteins, which mainly associated with purine-related nucleotide binding and purine ribonucleotide binding (Figure 3B). Expression of actin cytoskeletal proteins is specifically expressed in fibroblasts and promotes the process of joint fibrosis [41]. Cellular component analysis of the differentially expressed proteins also showed that these differential proteins were involved in the regulatory functions of contractile fibers, myofibrils, contractile fibers and sarcomeres (Figure 3C). HOPP treatment may therefore primarily affect functional clusters of fibrotic proteins to enhance joint recovery. Prine nucleoside phosphorylase converts guanosine to guanine, inosine to hypoxanthine, and 2'-deoxyguanosine to guanine, and results in the downstream formation of prooxidants and vasotoxicity of hypoxanthine and xanthine. In a study of treating sickle cell disease mice with 8-aminoguanine, a highly efficient purine nucleoside phosphorylase inhibitor, Tofovic et al. found that 8-aminoguanine treatment not only significantly alleviated anemia, but also significantly reduced left ventricular, right ventricular hypertrophy and hepatosplenomegaly. Pathological analysis showed that 8-aminoguanine significantly alleviated fibrotic damage [42]. Indeed, during HOPP treatment, many differentially expressed purine nucleotide-binding proteins and purine ribonucleotide-binding proteins were significantly altered, which may include purine nucleosides phosphorylase-related factors. It suggests that HOPP may support ankle joint recovery through its effects on purine nucleoside phosphorylase. In addition, we noticed that 4% of the significantly differentially expressed proteins belong to the calmodulin-binding proteins (Figure 3B), which are important for the function of mastocytes [43]. A previous study reported that mastocytes are associated with fibroblasts in arthrofibrosis. Clinical trials provided evidence that inhibition of mastocytes can efficiently reduce fibroblast proliferation [44]. Therefore, HOPP treatment may also influence calcium metabolism in mastocytes to reduce the proliferation of fibroblasts. The cellular component analysis (Figure 3C) showed that 17% of the differentially expressed proteins were located in fibers or fibrous parts, 19% of the differentially expressed proteins were cytoskeletal proteins, and 39% of the differentially expressed proteins were located in non-membrane–bound organelles. These data further indicates that a close relationship exists between HOPP treatment and the alteration of fibers, cytoskeletal structures, and non-membrane–bound organelles.

Recovery from fracture and ankylosis is long process. The analyses of pathway enrichment, protein cluster function enrichment, and the associated protein network provide valuable information for determining which protein clusters and pathways are responsible for the recovery and which proteins are key regulators or nodes for the processes involved in healing. On day seven after HOPP treatment, which may represent an early time point in the response to HOPP (Figure 4A), the data showed that most of the identified pathways, including calcium signaling, Integrin-Linked Kinase (ILK) signaling, and other proliferation-promoting regulatory pathways as well as the glycolysis I pathway, were downregulated. Calcium signaling is often a second messenger involved in neuronal transmission, fertilization,

cell growth, neurogenesis, learning and memory, and salivation. It also participates muscle contraction, cell movement, apoptosis, and regulation of cytoskeleton [45-47]. ILK is reported to involve multiple cellular functions including cell migration, proliferation, and adhesion [48,49] Glycolysis process is involved in regulating pro-inflammatory responses [50]. Thus, down regulation of those pathways at 7th day after HOPP treatment is benefit for inflammation and fibrosis control.

In contrast to the results after 7 days of HOPP treatment, after 14 days of treatment, differentially expressed proteins related to calcium signaling, ILK signaling, and epithelial adherents junction signaling were upregulated. The reversal of these signal pathways may be a response of the body to balance the early HOPP's anti-tissue inflammation and anti-fibrosis effects. Indeed, by 21 days of HOPP treatment, these differences in signaling pathways disappeared, which seems to support this hypothesis. After 21 days of HOPP treatment, most of the differential protein functional pathways that appeared after 7 to 14 days of HOPP treatment have tended to disappear. The main functional pathways were increased liver fibrosis/ hepatic stellate cell activation pathway, downregulation of protein ubiquitination pathway, upregulation of epithelial adhesion junction signaling pathway, upregulation of epithelial aldosterone signaling pathway, and upregulation of Cdc signaling pathway (Figure 6). We note that Chen et al. found in their study of treating liver cirrhosis with Ganoderma Lucidum Polysaccharide (GLP) that GLP exerted an anti-fibrotic effect by inducing the activation of Hepatic Stellate Cells (HSC) [51]. Tripathi et al., in their study of Homocysteine (Hcy) -induced liver fibrosis in Non-Alcoholic Steatohepatitis (NASH), found that multiple liver proteins are ubiquitinated in NASH [52]. Downregulation of the protein ubiquitination pathway is beneficial to the anti-fibrotic process. On the other hand, the upregulation of the hepatic fibrosis, aldosterone signaling pathway [53], and the Cdc42 signaling pathway [54], in epithelial cells further promote the trend of fibrosis. This paradoxical regulation of fibrosis should depend on the ultimate balance between the two aspects of regulation. Elevated epithelial adherens junction signaling pathways may be related to tissue re-modeling during tissue repair.

Function analysis provided similar information to pathway analysis from another perspective. After HOPP treatment for 7 days, proteins related to calmodulin and muscle contraction were markedly downregulated (Figure 4B), whereas after 14 days of treatment, almost all of these proteins were upregulated (Figure 5B). Then after 21 days of treatment, the expression levels of these proteins in the HOPP treatment group were nearly the same at those in the control group (Figure 6B). These results suggest that, at the molecular level, HOPP treatment mediated highly dynamic changes in the expression of skeletal proteins to promote recovery from injury.

Network analysis further identified the key proteins involved in the ankylosis recovery process. From the network analysis conducted after 7 days of HOPP treatment (Figure 4C), we identified a potentially important regulatory network connecting energy metabolism, gene expression, cytoskeletal regulation, signal transduction, and collagen degradation. In this network, dynamic alteration of myosin leads to alteration of the cytoskeleton and thereby inhibits the motility of fibroblasts [55]. In addition, the ERK1/2 signaling pathway may play an important role in early recovery processes by inducing the upregulation of Matrix Metalloproteinases (MMPs), which can degrade collagen [56], involving in cell motility. Essentially the same network was identified after both 7 and 14 days of HOPP treatment (Figure 5C), and at this stage, alteration of ATPase could be involved in both ATP synthesis and dynamic changes in myosin [57]. This would lead to not only the cytoskeletal changes, but also decreased energy metabolism, which results in the inhibition of fibroblast proliferation and motility. ATPase alteration and the ERK1/2 signaling pathway may act in combination to regulate the expression of MMPs and HMMR and support recovery from arthrofibrosis. After 21 days of HOPP treatment (Figure 6C), although the key factors in arthrofibrosis, such as collagen proteins, were not changed, two key cell cycle regulators, CSNK1G2 and PELO, were identified as significantly upregulated. Both CSNK1G2 and PELO can activate the cell cycle process and are related to collagen proteins under the mediation of Polyubiquitin C (UBC) [58]. These findings indicate that HOPP treatment may lose efficiency over time, and arthrofibrosis affects essentially all biological processes.

Conclusion

Based on the results discussed above, we propose a possible potent mechanism for the effects of HOPP treatment on ankylosis. HOPP treatment may involves various metabolic pathways to inhibit myosin-related cytoskeletal regulation to reduce the size of developing fibroblasts and promote fibroblast-populated collagen lattice contraction, limit calcium metabolism to control the proliferation of mastocytes, and deactivate energy metabolism processes to prevent cell cycle progression.

Our results provide further insight into the effects of HOPP in the healing of arthrofibrosis and tendon adhesions. We also identified some specific key regulators of arthrofibrosis, the cell cycle activator/regulator CSNK1G2 and PELO. Pathways related to the phosphatases, energy metabolism, calcium metabolism, myosin protein groups, and MAPK signaling pathways represented the most of the networks in our study. Thus, the HOPP-induced healing responses and the arthrofibrosis development processes are closely related to the protein phosphorylation system, which provides a new view for studies of HOPP. Moreover, many phosphorylated proteins may play critical roles in the HOPP-induced responses.

Ethics Approval and Consent to Participate

All protocols involving animals were approved by the Animal Ethics Committee of The First Teaching Hospital of Xinjiang Medical University (No: A-20080114012). All applicable international, national, and/or institutional guidelines for the care and use of animals were followed.

Availability of Data and Materials

The datasets generated and analyzed during the present study are available from the corresponding author on reasonable request.

Authors' Contributions

QB and JJ: Conceived and designed the study, obtained research funding, supervised the project, interpreted the data, revised the manuscript, and approved the final version.

JT: Performed quantitative proteomic data analysis and provided bioinformatics support.

YY, WA, and HA: Participated in the study design, data collection, and experimental coordination.

BD, JA, and SN: Established the animal models and conducted

the animal experiments.

AM and TT: Prepared horse oil and participated in experimental procedures.

YA and AA: Contributed to project application and acquisition of research funding.

YN: Assisted in data interpretation, statistical analysis, and manuscript preparation.

All Authors: Reviewed the manuscript, contributed to the discussion of the results, and approved the final manuscript.

Acknowledgment

We are grateful to Hong Jin (PhD, Associate Professor), Pengyuan Yang (PhD, Professor), Fenying Yang (Senior Lab Technician), and Lei Zhang, Xinwen Zhou (Senior Lab Engineer) of the Centre of Proteomics and Systems Biology, Institutes of Biomedical Sciences, Fudan University, Shanghai, for identified using isobaric tags for relative and absolute quantification tandem mass spectrometry and bioinformatics analysis of the quantitative proteomic data.

References

1. Linklater JM, Fessa CK. Imaging findings in arthrofibrosis of the ankle and foot. Semin Musculoskelet Radiol. 2012;16(3):185-91.
2. Haller JM, Holt DC, McFadden ML, Higgins TF, Kubiak EN. Arthrofibrosis of the knee following a fracture of the tibial plateau. Bone Joint J. 2015;97-B(1):109-14.
3. Sayre LA. A new operation for artificial hip joint in bony anchylosis. Clin Orthop Relat Res. 1994;(298):4-7.
4. Holguin PH, Rico AA, Garcia JP, Del Rio JL. Elbow anchylosis due to postburn heterotopic ossification. J Burn Care Rehabil. 1996;17(2):150-4.
5. Barlow JD, Hartzler RU, Abdel MP, Morrey ME, An KN, Steinmann SP, et al. Surgical capsular release reduces flexion contracture in a rabbit model of arthrofibrosis. J Orthop Res. 2013;31(10):1529-32.
6. Mayr HO, Stöhr A. Arthroscopic treatment of arthrofibrosis after ACL reconstruction: Local and generalized arthrofibrosis. Oper Orthop Traumatol. 2014;26(1):7-18.
7. Borges PRT, Procopio PRS, Chelidonopoulos JHD, Zambelli R, Ocarino JM, et al. "Passive stiffness of the ankle and plantar flexor muscle performance after Achilles tendon repair: A cross-sectional study." Braz J Phys Ther. 2017;21(1):51-7.
8. Dekker RG, Qin C, Lawton C, Muriuki MG, Havey RM, Alshouli M, et al. "Republication of "A biomechanical comparison of limited open versus Krackow repair for Achilles tendon rupture". Foot Ankle Orthop. 2023;8(3):24730114231188112.
9. Freedman BR, Salka NS, Morris TR, Bhatt PR, Pardes AM, Gordo JA. et al. "Temporal healing of achilles tendons after injury in rodents depends on surgical treatment and activity." J Am Acad Orthop Surg. 2017;25(9):635-47.
10. Yuanzhi LFLJZ. The Smoke-washing therapy with traditional Chinese medicine to postoperative ankylosis of fracture of elbow. Chin J Clin Rehabil. 2002;6:1215-6.
11. Manatbieke. Essence of Kazakh medicine. First Edition, Kuituno: Yili People's Publishing House. 1997;6:49-52.
12. Акпбков. Reads the people's oath [M]. Almaty: L: Hot Wasp. ввк53.59 X17, 62-6.
13. Zhang XP, Hua L, Shi QH, Yang ZL, Sun JJXAS. Study on permeability of horse fat. 2010.
14. Aishan J. Discussion about the experience on Kazakh traditional medicine for treatment of chronic shoulder dislocation. Chin Clin Med Month. 2002;1:193-4.
15. Baatibieke H. Kazakh traditional therapeutic medicine horse fat for treatment of chronic elbow dislocation. Chin J Ethnomed Ethnomed. 1996;13-4.
16. Yin Z, Jiangaguli A, Bone HJCJ, Injury J. Effect of horse-fat of Kazakh-medicine on SD-rat ankle-join ankylosis. 2011.
17. Kim IW, Jeong HS, Yun HY, Baek KJ, Kwon NS, Kim DS. Efficacy of horse oil on lipopolysaccharide-induced inflammation in human keratinocyte. J Tradit Chin Med. 2021;41(3):355-9.
18. Goik U, Goik T, Zaska I. The Properties and application of argan oil in cosmetology. Eur J Lipid Sci Technol. 2019;121(4):1800313.
19. Piao MJ, Kang KA, Zhen AX, Kang HK, Koh YS, Kim BS, et al. Horse oil mitigates oxidative damage to human HaCaT keratinocytes caused by ultraviolet B irradiation. Int J Mol Sci. 2019;20(6):1490.
20. Nurbahet S, Bahedulet A. The introduction to Kazakh medicine [M]. In: Qian YG, editor. Beijing: Chinese Ancient Books Publishing House, First Edition. 2010:2-4.
21. Qianman B, Jialihasi A, Asilehan B, Kubai A, Aibek R, Wupuer A, et al. Active exercise promotes Achilles tendon healing and is accompanied by the upregulation of collapsin response mediator protein-2 in rats. Mol Med Rep. 2017;16(3):2355-60.
22. Nuerai S, Ainuer J, Jiasharete J, Darebai R, Kayrat A, Tang B, et al. Kazakh therapy on differential protein expression of Achilles tendon healing in a 7-day postoperative rabbit model. J Tradit Chin Med. 2011;31(4):367-75.
23. Wei T. Study on the effect of horse fat and skin penetration mechanism in Xinjiang. Xinjiang Medical University. 2014.
24. Jianguo YSLXMDZ. Study on supercritical Co_2 fluid extraction and the rheological properties and storage quality of horse fat. J Agric Products Process. 2008;12:64-6.
25. Wenjun W. Study on supercritical Co_2 fluid extraction and the rheological properties and storage quality of horse fat. Xinjiang Agricultural University. 2016.
26. Warmuth V, Eriksson A, Bower MA, Barker G, Barrett E, Hanks BK, et al. et al. Reconstructing the origin and spread of horse domestication in the Eurasian steppe. Proceedings of the National Academy of Sciences of the United States of America. 2012;109(21):8202-6.
27. Outram AK, Stear NA, Bendrey R, Olsen S, Kasparov A, Zaibert V, et al. The earliest horse harnessing and milking. Science. 2009;323(5919):1332-5.
28. Campone L, Celano R, Lisa Piccinelli A, Pagano I, Carabetta S, Sanzo RD, et al. Response surface methodology to optimize supercritical carbon dioxide/co-solvent extraction of brown onion skin by-product as source of nutraceutical compounds. Food Chem. 2018;269:495-502.
29. Qianman B, Wupuer A, Jiasharete T, Luo B, Nihemaiti M, Jielile J. iTRAQ-based proteomics reveals potential markers and treatment pathways for acute Achilles tendon rupture. J Orthop Surg Res. 2023;18(1):852. Link: https://pubmed.ncbi.nlm.nih.gov/37946221/
30. He Y, Lin J, Tang J, Yu Z, Ou Q, Lin J. iTRAQ-based proteomic analysis of differentially expressed proteins in sera of seronegative and seropositive rheumatoid arthritis patients. J Clin Lab Anal. 2022;36(1):e24133. Link: https://pubmed.ncbi.nlm.nih.gov/34812532/
31. Qianman B, Jiasharete T, Badalihan A, Mamately A, Yeerbo N, Bahesutihan Y, Wupuer A, Aisaiding A, Wuerliebieke J, Jialihasi A, Li P, Jielile J. iTRAQ-Based Proteomic Analysis of Spontaneous Achilles Tendon Rupture. J Proteome Res. 2025 Jan 3;24(1):65-76.
32. Qianman B, Jiasharete T, Wupuer A, Tuerxun A, Jialihasi A, Mamately A, Yeerbo N, Shawutali N, Badalihan A, Aisaiding A, Redati D, Wuerliebieke

J, Aizezi A, Bahesutihan Y, Zhao B, Ainiwaer N, Jielile J. Serum and Urinary Proteomic Signatures Revealing Redox and Metabolic Dysregulation in Acute Achilles Tendon Rupture. Protein Pept Lett. 2025;32(6):437-450.

33. Jielile J, Asilehan B, Wupuer A, Qianman B, Jialihasi A, Tangkejie W, et al. Early ankle mobilization promotes healing in a rabbit model of achilles tendon rupture. Orthopedics. 2016;39(1):e117-26.

34. Kambiranda D, Katam R, Basha SM, Siebert S. iTRAQ-based quantitative proteomics of developing and ripening muscadine grape berry. J Proteome Res. 2014;13(2):555-69.

35. Jielile J, Aibai M, Sabirhazi G, Shawutali N, Tangkejie W, Badelhan A, et al. Active Achilles tendon kinesitherapy accelerates Achilles tendon repair by promoting neurite regeneration. Neural Regen Res. 2012;7(35):2801-10.

36. Jialili A, Jielile J, Abudoureyimu S, Sabirhazi G, Redati D, Bai JP, et al. Differentially expressed proteins on postoperative 3 days healing in rabbit Achilles tendon rupture model after early kinesitherapy. Chin J Traumatol. 2011;14(2):84-91.

37. Rydén M, Önnerfjord P. *In vitro* models and proteomics in osteoarthritis research. Adv Exp Med Biol. 2023;1402:57-68.

38. Zhang Y, Xie J, Wen S, Cao P, Xiao W, Zhu J, et al. Evaluating the causal effect of circulating proteome on the risk of osteoarthritis-related traits. Ann Rheum Dis. 2023;82(12):1606-17.

39. Bahney CS, Zondervan RL, Allison P, Alekos Theologis A, Ashley JS, Ahn J, et al. Cellular biology of fracture healing. J Orthop Res. 2019;37(1):35-50.

40. Zhu L, Zhao Q, Yang T, Ding W, Zhao Y. Cellular metabolism and macrophage functional polarization. International reviews of immunology. Int Rev Immunol. 2015;34(1):82-100.

41. Hironaka T, Takizawa N, Yamauchi Y, Horii Y, Nakaya M. The well-developed actin cytoskeleton and Cthrc1 expression by actin-binding protein Drebrin in myofibroblasts promote cardiac and hepatic fibrosis. J Biol Chem. 2023;299(3):102934.

42. Stevan P, Tofovic EK, Jackson LL, Stephanie M, Enrico MN. Purine nucleoside phosphorylase inhibition attenuates the progression of anemia and organ damage in sickle cell mice. Blood. 2022;140(Suppl 1):2519-20.

43. Honda T, Nishio Y, Sakai H, Asagiri L, Yoshimura K, Inui M, et al. Calcium/calmodulin-dependent regulation of Rac GTPases and Akt in histamine-induced chemotaxis of mast cells. Cell Signal. 2021;83:109973.

44. Monument MJ, Hart DA, Salo PT, Befus AD, Hildebrand KA. Neuroinflammatory mechanisms of connective tissue fibrosis: Targeting neurogenic and mast cell contributions. Adv Wound Care (New Rochelle). 2015;4(3):137-51.

45. Rash BG, Ackman JB, Rakic P. Bidirectional radial Ca(2+) activity regulates neurogenesis and migration during early cortical column formation. Sci Adv. 2016;2(2):e1501733.

46. Berridge MJ, Lipp P, Bootman MD. The versatility and universality of calcium signaling. Nature reviews. Nat Rev Mol Cell Biol. 2000;1(1):11-21.

47. Joseph SK, Hajnóczky G. IP3 receptors in cell survival and apoptosis: Ca2+ release and beyond. Apoptosis. 2007;12(5):951-68.

48. Popescu SC, Brauer EK, Dimlioglu G, Popescu GV. Insights into the structure, function, and ion-mediated signaling pathways transduced by plant integrin-linked kinases. Front Plant Sci. 2017;8:376.

49. Dwivedi A, Sala-Newby GB, George SJ. Regulation of cell-matrix contacts and beta-catenin signaling in VSMC by integrin-linked kinase: Implications for intimal thickening. Basic Res Cardiol. 2008;103(3):244-56.

50. Saaoud F, Liu L, Xu K, Cueto R, Shao Y, Lu Y, et al. Aorta- and liver-generated TMAO enhances trained immunity for increased inflammation via ER stress/mitochondrial ROS/glycolysis pathways. JCI Insight. 2023;8(1):e158183.

51. Chen C, Chen J, Wang Y, Fang L, Guo C, Sang T, et al. Ganoderma lucidum polysaccharide inhibits HSC activation and liver fibrosis via targeting inflammation, apoptosis, cell cycle, and ECM-receptor interaction mediated by TGF-β/Smad signaling. Phytomedicine. 2023;110:154626.

52. Tripathi M, Singh BK, Zhou J, Tikno K, Widjaja A, Sandireddy R, et al. Vitamin B(12) and folate decrease inflammation and fibrosis in NASH by preventing syntaxin 17 homocysteinylation. J Hepatol. 2022;77(5):1246-55.

53. Munro R, Dorman D, Daley D, Tomlinson P. Meningococcal serogroups in New South Wales, 1977-1987. Med J Aust. 1988;149(7):360-2.

54. Hu X, Gan L, Tang Z, Lin R, Liang Z, Li F, et al. A natural small molecule mitigates kidney fibrosis by targeting Cdc42-mediated GSK-3β/β-catenin signaling. Adv Sci (Weinh). 2024;11(13):e2307850.

55. Schäfer A, Radmacher M. Influence of myosin II activity on stiffness of fibroblast cells. Acta Biomater. 2005;1(3):273-80.

56. Dragsbæk K, Neergaard JS, Hansen HB, Byrjalsen I, Alexandersen P, Kehlet SN, et al. Matrix metalloproteinase mediated type I collagen degradation - An independent risk factor for mortality in women. EBioMedicine. 2015;2(7):723-9.

57. Bolognani G, Majni M, Costato MM. ATPase and ATPsynthetase activity in myosin exposed to low power laser and pulsed electromagnetic fields. Bioelectrochem Bioenerg. 1993;32(2):155-64.

58. Ryu KY, Maehr R, Gilchrist CA, Long MA, Bouley DM, Mueller B, et al. The mouse polyubiquitin gene UbC is essential for fetal liver development, cell-cycle progression and stress tolerance. EMBO J. 2007;26(11):2693-706.